Plasmonic nanodevice with magnetic funcionalities: Fabrication and characterization

F. GALVEZ,[1] J. DEL VALLE,[1] A. GOMEZ,[1,2] M. R. OSORIO,[3] D. GRANADOS,[3] D. PÉREZ DE LARA,[3] M. A. GARCÍA,[4,5],* AND J. L. VICENT,[1,3]

[1]*Dpto. de Física de Materiales, Universidad Complutense de Madrid, 28040 Madrid, Spain*
[2]*Centro de Astrobiología, INTA-CSIC, E-28850 Madrid, Spain*
[3]*IMDEA-Nanociencia, Universidad Autónoma de Madrid, Cantoblanco, 28049 Madrid, Spain*
[4]*Instituto de Cerámica y Vidrio, Consejo Superior de Investigaciones Científicas, 28049 Madrid, Spain*
[5] *Instituto de Magnetismo Aplicado 'Salvador Velayos', Universidad Complutense de Madrid, 28230 Madrid, Spain*
magarcia@icv.csic.es

Abstract: We have designed and fabricated a nanodevice exhibiting simultaneously ferromagnetic properties of nanostructures with plasmonic properties of continuous films. Our device consists in an array of nanomagnets on top of a continuous plasmonic film. The patterned nanomagnets magnetic state is single domain and well-defined shape anisotropy. Despite the presence of the patterned media on top of the Au film, the system exhibit surface plasmon resonance characteristic of a continuous film, i. e., propagating surface plasmon-polaritons.

OCIS codes: (240.6680) Surface plasmons; (160.3820) Magneto-optical materials.

References and links

1. C. A. Ross "Patterned magnetic recording media" Annu. Rev. Mater. Res. **31**, 203-235 (2001).
2. C. A. Ross, H. I. Smith, T. Savas, M. Schattenburg, M. Farhoud, M. Hwang, M. Walsh, M. C. Abraham and R. J. Ram R J "Fabrication of patterned media for high density magnetic storage" J. Vac. Sci. Technol. B **17**, 3168-3176 (1999).
3. T. Jungwirth, J. Wunderlich and K. Olejník "Spin Hall effect devices" Nature Materials **11**, 382-390 (2012).
4. P. R.Hammar,B. R. Bennett, M. J. Yang and M. Johnson "Observation of Spin Injection at a Ferromagnet-Semiconductor Interface" Phys. Rev. Lett. **83**, 203 (1999).
5. J. F. Gregg, I. Petej, E. Jouguelet and C. Dennis " Spin electronics—a review" J. Phys. D: Appl. Phys. **35**, R121-R155 (2002).
6. W. L. Barnes, A. Dereux and T. W. Ebbesen "Surface plasmon subwavelength optics" Nature **424**, 824-830 (2003).
7. J. A. Schuller, E. S. Barnard, W. Cai,Y. Chul Jun, J. S. Whiteand M. L. Brongersma "Plasmonics for extreme light concentration and manipulation" Nature Mat. **9**, 193-204 (2010).
8. G. Armelles, A. Cebollada, A. García-Martíand M. U. González "Magnetoplasmonics: Combining Magnetic and Plasmonic Functionalities" Adv. Opt. Mat **1**, 10-35 (2013).
9. V. Temnov, G. Armelles, U. Woggon, D. Guzatov, A. Cebollada, A. Garcia-Martin, J. M. Garcia-Martin, T. Thomay, A. Leitenstorfer and R. Bratschitsch "Active magneto-plasmonics in hybrid metal–ferromagnet structures" Nature Photonics **4**, 107-111 (2010).
10. J. B. González-Díaz, A. García-Martín, J. M. García-Martín, A. Cebollada, G. Armelles, B. Sepúlveda, Y. Alaverdyan and M. Käll "Plasmonic Au/Co/Au Nanosandwiches with Enhanced Magneto-optical Activity" Small **4** 202-205 (2008).
11. V. I. Belotelov, I. A. Akimov, M. Pohl,V. A. Kotov,S. Kasture, A. S. Vengurlekar, A. Venu Gopal,D. R. Yakovlev, A. K. Zvezdinand M. Bayer "Enhanced magneto-optical effects in magnetoplasmonic" crystals Nature Nanotech. **6**, 370-376 (2011).
12. E. Ferreiro-Vila, J. B. González-Díaz, R. Fermento, M. U. González, A. García-Martín, J. M. García-Martín, A. Cebollada, G. Armelles, D. Meneses-Rodríguez and E. Muñoz Sandoval "Intertwined magneto-optical and plasmonic effects in Ag/Co/Ag layered structures" Phys. Rev. B **80**, 125132 (2009).

13. G. A. Wurtz, W. Hendren, R. Pollard, R. Atkinson, L. Le Guyader, A. Kirilyuk, T. Rasing, I. I. Smolyaninov and A. v. Zayats "Controlling optical transmission through magneto-plasmonic crystals with an external magnetic field" New J. Phys. **10**, 105012 (2008).
14. J. Chen , P. Albella , Z. Pirzadeh , P. Alonso-González, F. Huth , S. Bonetti , V. Bonanni , J. Akerman , J. Nogués , P. Vavassori , A. Dmitriev , J. Aizpurua and Rainer Hillenbrand "Plasmonic Nickel Nanoantennas" Small **7**, 2341-2437 (2011).
15. N. Maccaferri, A. Berger, S. Bonetti, V. Bonanni, M. Kataja, Q. H. Qin, S. van Dijken, Z. Pirzadeh, A. Dmitriev, J. Nogues, J. Akerman and P. Vavassori "Tuning the Magneto-Optical Response of Nanosize Ferromagnetic Ni Disks Using the Phase of Localized Plasmons" Phys. Rev. Lett **111**, 167401 (2013).
16. K. Lodewijks, N. Maccaferri, T. Pakizeh, R. K. Dumas, I. Zubritskaya, J. Akerman, P. Vavassori and A. Dmitriev "Magnetoplasmonic Design Rules for Active Magneto-Optics" Nano Lett. 14 7207-7214 (2014)
17. N. Maccaferri, K. E. Gregorczyk, T. V.A.G. de Oliveira, M. Kataja, S. van Dijken, Z. Pirzadeh, A. Dmitriev, J. Åkerman, M. Knez and P. Vavassori "Ultrasensitive and label-free molecular-level detection enabled by light phase control in magnetoplasmonic nanoantennas" Nature Commun. **6**, 6150 (2015).
18. M. Rollinger, P. Thielen, E. Melander, E. Ostman, V. Kapaklis, B. Obry, M. Cinchetti, A. García-Martín, M. Aeschlimann and E. Th. Papaioannou "Light Localization and Magneto-Optic Enhancement in Ni Antidot Arrays" Nano Lett. 16 2432 (2016)
19. N. Maccaferri, L. Bergamini, M. Pancaldi, M. K. Schmidt, M. Kataja, S. van Dijken, N. Zabala, J. Aizpurua and P. Vavassori "Anisotropic Nanoantenna-Based Magnetoplasmonic Crystals for Highly Enhanced and Tunable Magneto-Optical Activity" Nano Lett. **16,** 2533-2542 (2016).
20. M. Kataja, S. Pourjama, N. Maccaferri, P. Vavassori, T. K. Hakala, M, J. Huttunen, P, Törmä and S, van Dijken "Hybrid plasmonic lattices with tunable magneto-optical activity" Opt. Express 24, 3652 (2016).
21. L. Chen, J. Gao, W. Xia, S. Zhang, S. Tang, W. Zhang, D. Li, X. Wu and Y. Du "Tunable Fano resonance and magneto-optical response in magnetoplasmonic structure fabricated by pure ferromagnetic metals" Phys. Rev. B **93**, 214411 (2016).
22. N. Maccaferri, X. Inchausti, A. García-Martín, J. C. Cuevas, D. Tripathy, A. O. Adeyeye and P. Vavassori "Resonant Enhancement of Magneto-Optical Activity Induced by Surface Plasmon Polariton Modes Coupling in 2D Magnetoplasmonic Crystals" ACS Photonics **2**, 1769 (2015).
23. H. Raether, *Surface Plasmons on Smooth and Rough Surfaces* (Springer ,1986).
24. Y. Lee, M. A. Garcia, N. A. Frey Huls and S. Sun "Synthetic Tuning of the Catalytic Properties of Au-Fe_3O_4 Nanoparticles" Angew. Chem. **49**, 1271-1274 (2010).
25. S. Chandra, N. A. Frey Huls, M. H. Phan, S. Srinath, M. A. Garcia, Y. Lee, C. Wang, S. Sun, O. Iglesiasand S. Srikanth "Exchange bias effect in Au-Fe_3O_4 nanocomposites" Nanotechnology **25**, 055702 (2014).
26. H. Y. Park, M. J. Schadt, Lingyan , I. I. S Lim, P. N. Njoki, S. H. Kim, M. Y. Jang, J. Luo and C. J. Zhong "Fabrication of Magnetic Core@Shell Fe Oxide@Au Nanoparticles for Interfacial Bioactivity and Bio-separation" Langmuir **23**, 9050-9056 (2007).
27. J. L. Lyon, D. A. Fleming, M. B. Stone, P. Schiffer and M. E. Williams "Synthesis of Fe Oxide Core/Au Shell Nanoparticles by Iterative Hydroxylamine Seeding" Nano Lett. **4**, 719-723 (2004).
28. F. Bao, J. F. Li, B. Ren, J. L. Yao, R. A. Gu and Z. Q. Tian "Synthesis and Characterization of Au@Co and Au@Ni Core−Shell Nanoparticles and Their Applications in Surface-Enhanced Raman Spectroscopy" J. Phys. Chem. C **112**, 345-350 (2008).
29. D. Martín-Becerra, V. V. Temnov, T. Thomay, A. Leitenstorfer, R. Bratschitsch, G. Armelles, A. García-Martín and M. U. González "Spectral dependence of the magnetic modulation of surface plasmon polaritons in noble/ferromagnetic/noble metal films" Phys. Rev. B **86**, 035118 (2012).
30. J. C. Banthi, D. Meneses-Rodriguez, F. Garcia, M. U. Gonzalez, A. Garcia-Martin, A. Cebollada and G. Armelles "High Magneto-Optical Activity and Low Optical Losses in Metal-Dielectric Au/Co/Au–SiO2 Magnetoplasmonic Nanodisks" Adv. Mat. **24**(10), OP36-OP41 (2012).
31. H. Y. Feng, F. Luo, D. Meneses-Rodriguez, G. Armelles and A. Cebollada "From disk to ring: Aspect ratio control of the magnetoplasmonic response in Au/Co/Au nanostructures fabricated by hole-mask colloidal lithography" Appl. Phys. Lett. **106**, 083105 (2015).
32. V. I. Safarov, V. A. Kosobukin, C. Hermann, G. Lampel, and J. Peretti "Magneto-optical Effects Enhanced by Surface Plasmons in Metallic Multilayer Films" Phys. Rev. Lett. **73**, 3584- 3587 (1994).
33. E. Ferreiro Vila, X. M. Bendana, J. B. González-Díaz, A. García-Martín, J. M. García-Martín, A. Cebollada, G. Armelles, D. Meneses and E. Muñoz-Sandoval "Surface plasmon resonance effects in the magneto-optical activity of Ag–Co–Ag trilayers" IEEE Trasn. Magn. **44**(11), 3303-3306 (2008).
34. G. Armelles, A. Cebollada, A. García-Martín, J. M. García-Martín, M. U. Gonzalez, J. B. González-Díaz, E. Ferreiro-Vila and J. F. Torrado "Magnetoplasmonic nanostructures: systems supporting both plasmonic and magnetic properties" J. Opt. A: Pure Appl. Opt. **11**, 114023 (2009).
35. D. Regatos, D. Fariña, A. Calle, A. Cebollada, B. Sepúlveda, G. Armelles and L. M. Lechuga "Au/Fe/Au multilayer transducers for magneto-optic surface plasmon resonance sensing" J. Appl. Phys. **108**, 054502 (2010).
36. B. Caballero, A. García-Martín and J. C. Cuevas "Hybrid Magnetoplasmonic Crystals Boost the Performance of Nanohole Arrays as Plasmonic Sensors" ACS Photonics **3**, 203-208 (2016).
37. E. Th. Papaioannou, T. Meyer, and B. Hillebrands "Magneto-optical enhancement in Co/Au patterned nanostructures" J. Surf. Interf. Mat. **2**, 40-45 (2014).

38. J. Mejia-Lopez, D. Altbir, A. H. Romero, X. Battle, I. V. Roshchin, C. P. Li and I. K. Schuller "Vortex state and effect of anisotropy in sub-100-nm magnetic nanodots" J. Appl. Phys. **100**, 104319 (2006).
39. A. Serrano, O. Rodriguez de la Fuente, M. A. García "Extended and localized surface plasmons in annealed Au films on glass substrates" J. Appl. Phys. **108**, 074303 (2010).
40. F. Galvez, C. Monton, A. Serrano, I. Valmianski, J. De la Venta, I. K. Schuller and M. A. Garcia "Effect of photodiode angular response on surface plasmon resonance measurements in the Kretschmann-Raether configuration" Rev. Sci. Instrum. **83**(9), 093102 (2012).
41. We simulated the spectra with the WINSPALL freeware code, see http://www.mpip-mainz.mpg.de/knoll/soft/ for WINSPALL freeware code.
42. J. M. Teixeira, R. Lusche, J. Ventura, R. Fermento, F. Carpinteiro, J. P. Araujo, J. B. Sousa, S. Cardoso and P. P. Freitas "Versatile, high sensitivity, and automatized angular dependent vectorial Kerr magnetometer for the analysis of nanostructured materials" Rev. Sci. Instrum. **82**, 043902 (2011).
43. A. Hubert and R. Schafer, *Magnetic domains: The analisis of magnetic microstructures* (Springer, 1998)
44. J. M. D. Coey, *Magnetism and Magnetic Materials* (Cambridge, Univ. Press, 2010)
45. M. J. Donahue and D. G.Porter "OOMKMF User's guide, Version 1", Interagency Report NISTIR 6376 (1999)
46. M. Grimsditch and P. Vavassori "The diffracted magneto-optic Kerr effect: what does it tell you?" J. Phys.C: Cond. Mat. **16**, R275-R294 (2004).
47. R. P. Cowburn "Property variation with shape in magnetic nanoelements" J. Phys. D: Appl. Phys. **33**, R1-R16 (2000).
48. B. D. Cullity and C. D. Graham, *Introduction to magnetic materials* (Willey 2009).
49. W. Knoll, "Interfaces and thin films as seen by bound electromagnetic waves" Annu. Rev. Phys. Chem. **49**, 569-638 (1998).
50. A. Kolomenski, A. Kolomenskii, J. Noel, S. Peng and H. Schuessler "Propagation length of surface plasmons in a metal film with roughness" Appl. Optics **48**, 5683-5691 (2009).
51. S. I. Bozhevolnyi, V. S. Volkov, E. Devaux and T. W. Ebbesen "Channel Plasmon-Polariton Guiding by Subwavelength Metal Grooves" Phys. Rev. Lett. **95**, 046802 (2005).
52. M. Born and E. Wolf, *Principles of Optics* (Pergamon Press, 1970)
53. P. Lalanne and M. Hutley, "The optical properties of artificial media structured at a subwavelength scale" in *Encyclopedia of Optical engineering* (Marcel Dekker, 2003)
54. T. C. Choy, *Effective Medium Theory: Principles and Applications* (Oxford, 2015)
55. G. A. Niklasson, C. G. Granqvist, O. and Hunderi "Effective medium models for the optical properties of inhomogeneous materials" Appl. Opt. **20**, 26-30 (1981).
56. U. Kreibig and M. Vollmer *Optical Properties of metal clusters* (Springer, 1995).
57. M. H. Tyboroski, N. R. Andersonand R. E. Camley "An effective medium study of surface plasmon polaritons in nanostructured gratings using attenuated total reflection" J. Appl. Phys. **115**, 013104 (2014).
58. X. Zhang and Y. Wu "Effective medium theory for anisotropic metamaterials" Sci. Rep. **5**, 7892 (2015).
59. H. S. Leong, J. Guo, R. G. Lindquistand Q. H. Liu "Surface plasmon resonance in nanostructured metal films under the Kretschmann configuration" J. Appl. Phys. **106**, 124314 (2009).
60. M. Mrejen, A. Israel, H. Taha, M. Palchan and A. Lewis "Near-field characterization of extraordinary optical transmission in sub-wavelength aperture arrays" Opt. Express **15**, 9129-9138 (2007).
61. P. B. Johnson and R. W. Christy "Optical Constants of the Noble Metals" Phys. Rev. B **6**, 4370 (1972).
62. R. L. Olmon, B. Slovick, T. W. Johnson, D. Shelton, S. H. Oh, G. D. Boreman and M. B. Raschke "Optical dielectric function of gold" Phys. Rev. B **86**, 235147 (2012).

1. Introduction

Magnetic nanomaterials have been used for many years in very different devices as memory elements [1,2] or more recently sources of spin polarized currents [3,4] spin filters [5] and others [6]. Simultaneously, plasmonic elements are included in circuits in order to use optical signals at sub-wavelength scales [6,7]. Therefore, mesostructures containing both magnetic and plasmonic elements, result interesting due to their potential uses for the development of new miniaturized devices [8-12] not only to use both technologies separately, but also in order to take advantage of the coupling phenomena between both effects [10,11,13].

Coexistence of intense plasmonic and strong ferromagnetic properties at room temperature in a single material is challenging. The surface plasmon resonance (SPR) is maximized in metals where the conduction electrons are highly decoupled from the atomic network so they behave as plasmonic matter. This condition is well achieved for noble metals as silver and gold which also present a high chemical stability that is required to avoid surface oxidation. On the other hand, ferromagnetic metals usually exhibit a strong interaction between localized spins and itinerant spins which leads to the macroscopic magnetic polarization. Hence, it is difficult to achieve ferromagnetic and plasmonic behaviors in the same material. Only recently,

nanostructures of Ni [14-20] Ni/Co [21] and permalloy antidots [22] have been reported to exhibit surface plasmons in combination with their well-known ferromagnetic character at room temperature. However, the intensity of the plasmonic resonance in these type of materials is fairly weaker than for noble metals as Au or Ag where the electromagnetic field can be increased locally up to 80 times upon excitation of surface plasmons [23].

An alternative approach to obtain magneto-plasmonic systems consists in developing nanostructures containing plasmonic and ferromagnetic elements. There are two great groups of hybrid magneto-plasmonic structures that have been widely explored.

The first one consists in hybrid structures where both the plasmonic and ferromagnetic elements are nanometric. In the last years, the recent advances in colloidal chemistry allowed to develop complex nanoparticles with ferromagnetic and plasmonic elements with different architectures as dimers [24], flowers [25] or core-shell structures [26-28] that exhibit ferromagnetic properties and surface plasmon resonances. Patterning of multilayers to form nanometric elements has been also studied, mainly in order to tune the SPR [29-31]. This type of structures exhibit localized surface plasmon resonance, while the ferromagnetic behavior can be tuned through the shape anisotropy.

The second type of magneto-plasmonic systems consist in ferromagnetic/plasmonic multilayers, patterned or continious, being the most explored configuration a thin ferromagnetic layer embedded in a plasmonic film [8,12,32-36]. This type of structures, present surface plasmon-polaritons propagating along the plasmonic metal surface. The shape anisotropy keeps the magnetization in plane but for continuous films or circular geometries there is no chance to have a well-defined shape anisotropy axis and consequently square hysteresis loops with large remanence.

Other configurations, as hybrid systems with one of the elements patterned and the other in form of continuous films have been scarcely explored and mainly of cussed on patterning the plasmonic element to excite localized SPR [34,37]. Very few systems with this structure present propagating surface plasmons [22,36] and those correspond to system where the ferromagnetic elements exhibit also weak surface plasmons resonance.

In this paper we present and characterize a new configuration of ferromagnetic/plasmonic system consisting on a mesoscopic pattern of ferromagnetic bars deposited on top of a continuous plasmonic film. The patterning of the ferromagnetic bars allows tuning their ferromagnetic behavior by choosing dimensions to exhibit large shape anisotropy and single domain behavior, so the magnetization of the individual nanomagnets is stable at room temperature. Although patterning of the media in contact with the plasmonic elements may yield to localized SPR, in our device, propagating surface plasmon-polaritons with relative weak damping are observed. In this system, the properties of mesomagnets coexist with propagating surface plasmon-polaritons.

2. Experimental

The analyzed sample is a continuous gold thin film with square arrays of permalloy (Py), Ni 80-Fe 20, nanobars on top of it. The substrate was 1mm thick BK7 glass cleaned with soapy water and isopropyl alcohol prior to the sample fabrication. A 50 nm thick gold film was directly grown on the glass substrate by physical vapor deposition of high-purity gold (99.99%) wires through an electron beam evaporator. On top of the gold film, electron beam lithography was used to pattern several identical arrays on a baked PMMA-A4 resist layer (200 nm thickness). Subsequently, 50 nm of Py, were deposited into these arrays by DC magnetron sputtering. Finally, we performed a lift-off process, so that only the Py nanobars arrays remained on the gold film. The nanobars dimensions were 150 nm for the short axis and 800 nm for the long axis with a periodicity of 500 nm and 1500 nm respectively, filling up to 75 μm x 75 μm arrays with 15 μm of separation for a total 400 arrays (Fig. 1). With these dimensions the magnetic interaction between the nanomagnets is negligible so they behave as isolated elements [38].

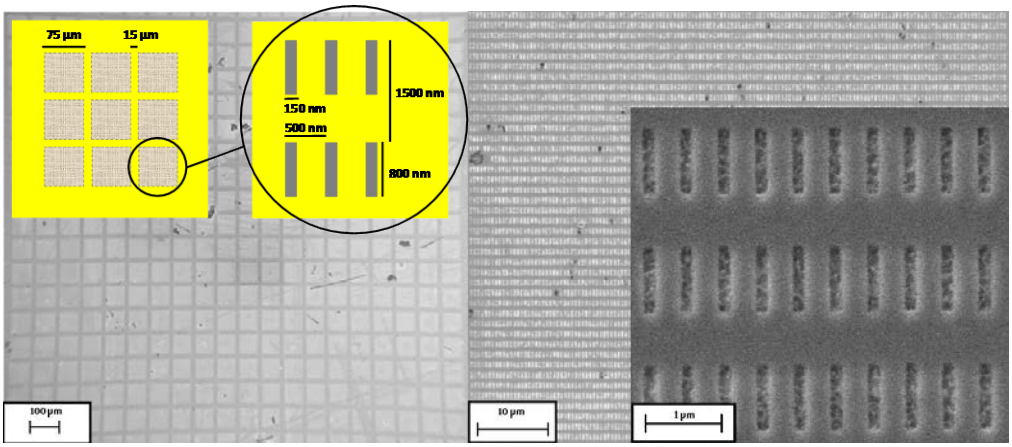

Fig. 1 SEM images of the full-size sample (left) with a scheme of the structure (left inset) and a close-up of one of the arrays (right) with a detail of the nanobars (right inset)

The SPR was measured using the Kretschmann-Raether configuration [23] with a homemade device described elsewhere [39]. A scheme of the set-up is depicted in figure 2a. SPR was excited using a 632.8 nm laser; the angular response of the photodiode was corrected as described in [40]. For each sample a minimum of 6 scans were recorded. The spectra we present correspond to the average of these scans where the symbol size indicates the standard deviation. Any possible drift in the motor positions was corrected by fixing the position of the critical angle to 42.6º; this value depends only on the glass refractive index and the surrounding air and it is independent of the Au film properties. SPR curve simulations were carried out using Winspall freeware by RES-TEC24 including the correction of the refraction for triangular prisms [41].

Magnetization curves were obtained with a home-made Kerr magnetometer in longitudinal configuration, i.e., with the magnetic field applied in the plane formed by the incident and reflected beams and parallel to the sample plane ([42-44]) as described in figure 2b. The system uses a 635 nm laser diode in p-polarization as light source. The laser beam was modulated at 313 Hz using a mechanical chopper and the signal analyzed with a lock-in amplifier tuned at this frequency. The reflected (m=0) and the diffracted beams (m=1) were used to record the magnetization curves. The incident beam was divided into two with a beam splitter in order to track the fluctuations of the incidence beam and compensate them by subtracting the incident signal from the reflected and diffracted ones after proper amplification.

Simulations for the magnetization loop of the individual array elements were performed using OOMMF freeware by NIST [45]. A cell size of 25 nm was used to simulate a single element with geometry and dimensions identical to those of the fabricated ones. The simulation was performed placing this element inside a variable longitudinal magnetic field ranging from 1 kOe to -1 kOe then to 1 kOe again in order to get a closed magnetization loop.

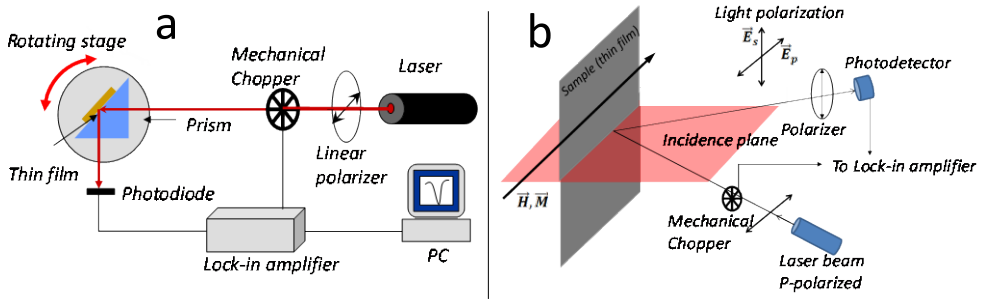

Fig 2. Schemes of the experimental set-ups used for (a) Longitudinal MOKE and (b) Surface plasmons resonance using the Kretschmann-Raether configuration

3. Results and discussion

3.1 Magnetic characterization

Figure 3 show the magnetization curves measured by Kerr technique in both the reflected (m=0) and diffracted (m=1) beams with the magnetic field applied along the bar axis. In both cases a square hysteresis loop is observed with remanence close to 100% and coercive field of about 400 Oe. The magnetization curve recorded in the diffracted beam shows a shoulder at the field inversion which is characteristic of curves obtained from the diffracted beam for non-interacting nanostructures. [46].

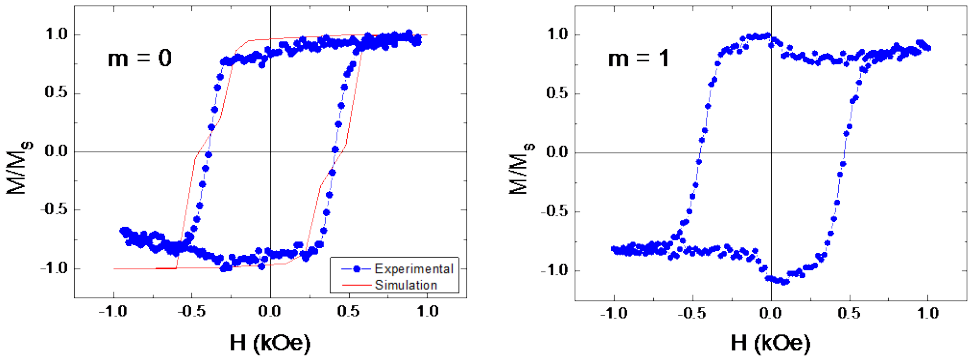

Fig. 3 Magnetization curves from the Au+Py bars measured by Kerr technique along the easy axis (a) at the reflected (m=0) and (b) at the first diffracted (m=1) beams.

In figure 3a we compare the experimental magnetization curve measured by Kerr technique in the reflected beam with the simulation performed using OOMMF for an individual Py bar. Both curves show a reasonable good agreement confirming that the dipolar interactions between the nanomagnets are negligible. The coercive field of the simulated curve is 450 Oe in comparison with the 400 Oe for the experimental one. Therefore, these nanostructures exhibit square hysteresis loops with steady magnetization at room temperature due to the shape anisotropy [47] which results remarkable in view of the potential applications in several field as information storage or spintronics. This high remanence is

consequence of the low magnetocrystalline anisotropy of permalloy (~10^3 J/m3) and large saturation magnetization ($8.3 \cdot 10^5$ A/m) as well as the large aspect ratio of the bars. In this situation, the shape anisotropy is two orders of magnitude larger than the magnetocrystalline one and the system exhibit high remanence in order to minimize magnetostatic energy.

Magnetization curves measured in the hard axis (not shown) presented very small remanence and coercivity but large saturation field (over 2 KOe) as expected for nanobars with large aspect ratio and saturation magnetization, and small magnetocrystalline anisotropy [48].

3.2 Optical characterization

Figure 4 shows the reflectivity spectra recorded at the bare Au and Au/Py bars regions of the samples measured for both directions of the SPR propagation vector, parallel and perpendicular to the bars main axis. All the spectra show a kink at 42.6º corresponding to the critical angle for total internal reflection [23,49].

The spectrum corresponding to the Au region shows reflectivity below 5% at extinction and a resonance angle at 47.5 deg. There are small differences between the spectra recorded in this bare Au region in the direction parallel and perpendicular to the bars main axis that are due to experimental errors and provide an estimation of the reproducibility of our measurements.

The profile of the curves measured at the nanobars region is that characteristic of surface plasmon polaritons in Au films. Thus, the presence of the mesomagnets does not lead to the extinction of surface plasmon polaritons. The reason is the existence of channels between the mesomagnets where the plasmons can travel almost freely.

These spectra shows reflectance at resonance of 43% and 49% for the excitation of SPR with propagation parallel and perpendicular to the bar main axis respectively. These values confirm that the resonance is relatively intense despite the presence of thick (50 nm) Py nanomagnets on top of the Au plasmonic film.

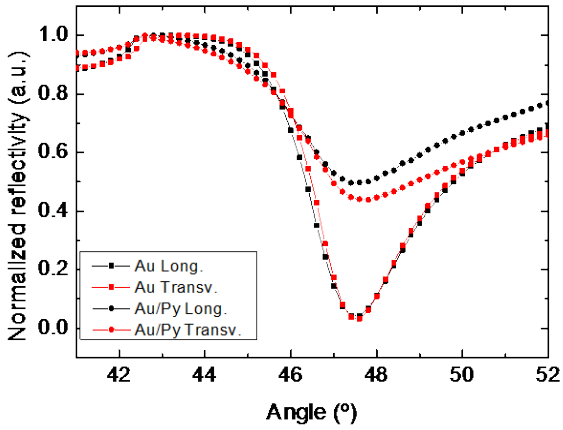

Fig. 4. Reflectivity spectra measured at the bare Au region and at the Py bars on top the Au film region with the wavevector of the SPR parallel and perpendicular to the axis of the bars.

This indicates that the surface plasmons propagating in the direction perpendicular to the Py bars have weaker damping than those propagating parallel to the bars. The area covered by Py is the same for both cases. Thus, the differences in the reflectivity spectra must be related to the damping induced by the Py on the surface plasmons propagating in the bare Au region of the sample. The propagation length of surface plasmon is of the order of micrometers, (that is, much larger than the distances of the pattern) even in presence of roughness [50]. Therefore, in our sample, the propagation of surface plasmons will take place mainly along the

"channels" between the bars. The width of these channels is 350 nm and 700 nm for the directions parallel and perpendicular to the bar axis respectively. Previous works [51] demonstrated that the propagation of surface plasmons along channels increases noticeably as the width of the channel reduces, explaining the differences we observe here between the curves measured in both directions.

3.3 Analysis of the optical properties

In order to analyze the interaction of the light with the sample we must consider the relative dimensions of the pattern and the plasmon wavelength. When the light interacts with a patterned medium there are two extreme situations named "long wavelength" and "short wavelength" ranges.

The short wavelength regime corresponds to the case where light wavelength is fairly smaller than the pattern dimensions. In this case, the light interacts with two different media and the result of the interaction (for instance the intensity of the reflected or transmitted light) is the sum of the interaction with each medium weighted by their relative areas. On the other hand, the long wavelength regime corresponds to media patterned with dimensions much shorter than the light wavelength. In this case, the light interaction with the matter can be analyzed as the interaction with an effective medium with a dielectric permittivity that is obtained from those of the individual elements of the pattern [52-54]. There is a large number of effective medium theories dedicated to determine the permittivity of the effective medium depending on the particular problem to analyze, being the simplest approximation to average the dielectric permittivity of the elements of the pattern weighted by their relative volumes [54-57].

A third intermediate situation corresponds to the case where the light wavelength is of the same order of the pattern dimension. In this case, a proper analysis of the light-matter interaction must be addressed by solving Maxwell equations. However, effective medium theories usually allow to describe the light-matter interaction in this range but with effective physical parameters that are not those well-defined for the extreme regimes of short and long wavelength approximation [58,59]. In particular, at this scale, interferences and resonant conditions can lead to resonances and sharp dependences of the optical properties with the pattern dimensions when the ratio between light wavelength and pattern dimensions is an integer number [60].

The wavelength of the laser used for excitation is 632 nm in air and the Au region resonance is achieved at about ~48 deg of incidence with a refractive index of the silica substrate of 1.52. Therefore, the wavevector of the surface plasmons in the Au film is about 680 nm [23].

Our patterned media have some dimension fairly smaller than this wavelength (150 nm width of the bars), other dimensions of the same order (500 nm bar distance and 800 nm bars length) and other that are fairly larger (the length of some channels in the material) so it is not clear what is the best framework for the analysis of the optical properties of our system. Therefore, we simulated the reflectivity spectra considering the three possible frameworks in order to determine their validity.

In our sample the Py bars cover the 11% of the area. Thus, we initially simulated the reflectivity spectrum for the sample as the sum of the 0.89 times spectrum of a bare Au film plus 0.11 of the spectrum of a 50nm Au/50 nm Py bilayer. This analysis should correspond to the short wavelength approximation and, as shown in figure 5a the result is very poor. In particular the simulated spectrum is much more similar to that of the Au film than the experimental ones, indicating that this procedure underestimates significantly the damping of the SPR because of the presence of the Py bars.

Subsequently, we simulated the SPR spectra assuming that we are in the large wavelength range, and considered a bilayer consisting on a 50 nm of Au plus a second layer also with 50 nm thickness and an effective dielectric permittivity. We used as effective permittivity the

average of the dielectric permittivity of the components of the films (Py and air) weighted by their relatives volumes, that is, ε_{eff}=0.11 ε_{Py}+0.89 ε_{air}, that results in ε_{eff} =1.132+i 0.352.

As figure 5b shows, neither in this case the results of the calculation matches the experimental data for both, SPR spectra measured in the direction longitudinal and perpendicular to the bars main axis, confirming that the large wavelength approximation is neither valid in this regime.

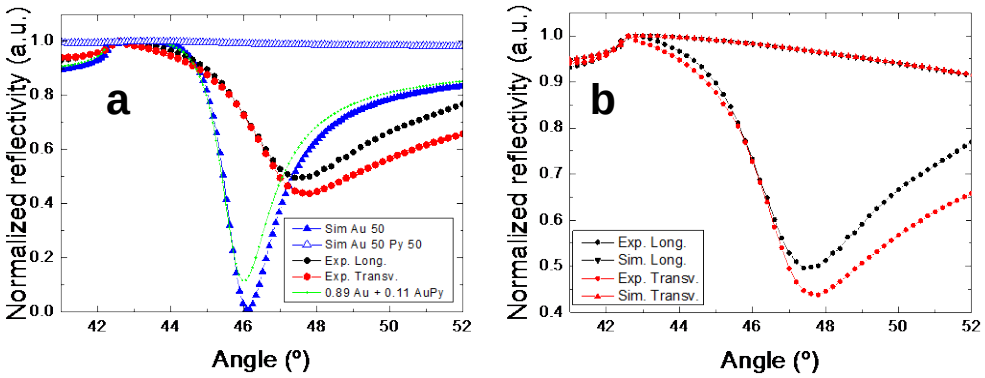

Figure 5. Experimental and simulations of the reflectivity spectra according to (a) the short wavelength and (b) large wavelength approximation as described in the text.

Finally, we tried to fit the SPR spectrum with an effective medium assuming a first 50 nm Au layer plus a second continuous one being its the thickness and dielectric permittivity free fitting parameters. To this purpose we initially fit the SPR spectra of the bare Au region (measured in a region of the sample away from the patterned one), considering as free parameters the thickness and dielectric function of the Au. The best fit corresponded to an Au thickness of 48.6 nm and a dielectric permittivity of ε=-9.11+i 3.03 as shown in figure 6a. The difference between the nominal thickness of the Au films (50 nm) and that obtained from the simulation is within the experimental error of the deposition thickness control system, while the dielectric function obtained from the simulation is close to that reported in literature for Au films at 632.8 nm [61,62]. Later we fitted the SPR spectrum of the Au film + Py bars region assuming a continuous bilayer, but fixing the thickness and dielectric permittivity of the first Au layer to those obtained in the previous fit (being free fitting parameters the thickness and dielectric function of the second layer). These fits, shown in figure 6b and 6c were optimized assuming the effective continuous top film to be 15.2 nm thick with ε=-9.0125+i 4.511 and 9.3 nm thick with ε=-7.472+i 7.585 for the spectra with the surface plasmon wave vector parallel and perpendicular to the bars axis respectively. These acceptable fits confirm that in this intermediate regime the system can be described macroscopically with an effective medium but with thickness and dielectric permittivity that does not follow the sum rules of the long wavelength approximation.

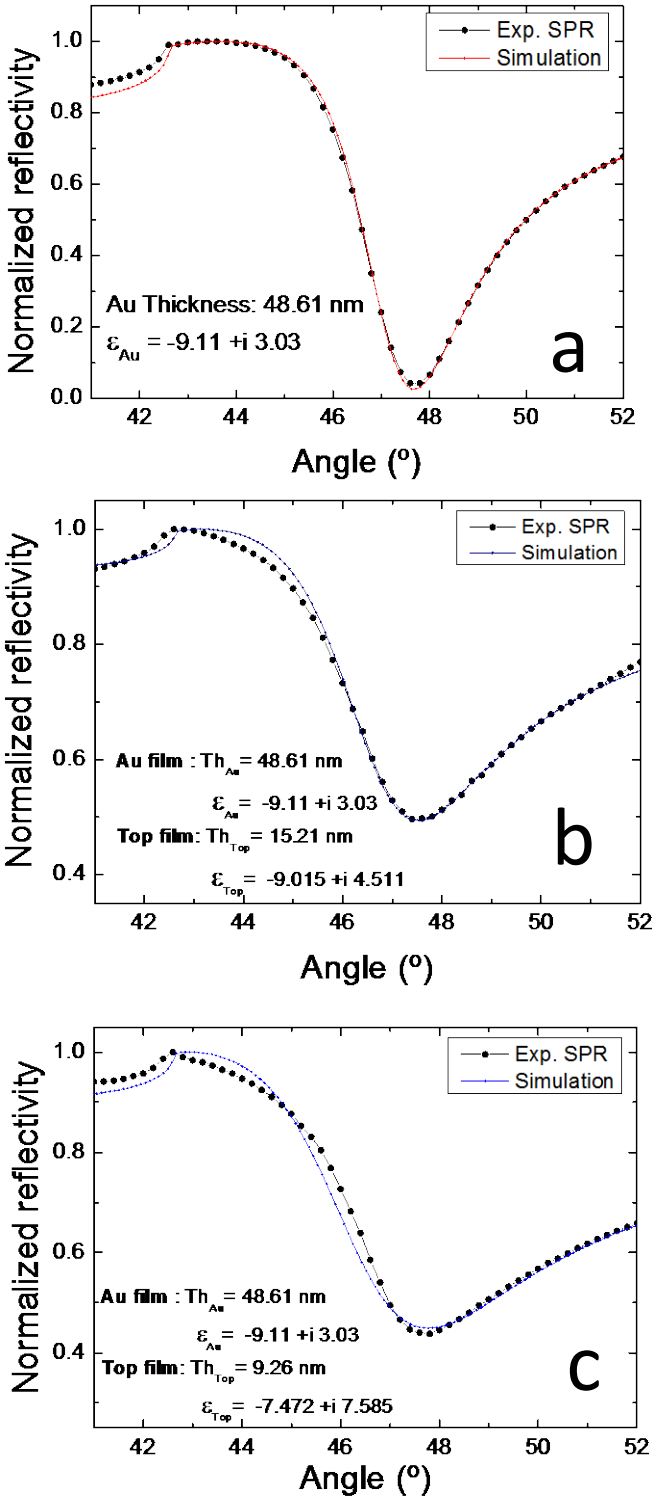

Figure 6. Fit of the SPR spectra of (a) bare Au region, and the region of Au+Py bars with the surface plasmon wavevector (b) parallel and (c) perpendicular to the bars axis.

4. Conclusions

In summary, we present a new configuration of nanostructures containing magnetic and plasmonic elements with direct contact consisting of patterned Py bars on top of a continuous Au film. The Py bars exhibit stable ferromagnetism at RT with Hc=400 Oe due to the well-defined shape anisotropy. Despite the presence of thick (50 nm) ferromagnetic nanostructures in direct contact with the Au film, the system exhibit propagating surface plasmons with intensity about 50% of that of a bare Au film. The plasmonic properties of the films are appropriately described by an effective medium although the parameters of such a medium cannot be derived straightforward from those of their elements.
Therefore, we developed a system where stable and intense ferromagnetic properties coexists with propagating surface plasmon-polaritons despite the discrete character of the structures with dimensions similar to surface plasmons wavelength.

Acknowledgments

This work has been supported by the Ministerio Español de Economia y Competitividad (MINECO) MAT2013-48009-C4-1 and FIS2013-45469-C4-1 and Comunidad de Madrid (CM) S2013/MIT-2850. D. G. acknowledges RYC-2012-09864, MAD2D-CM Program (S2013/MIT-3007) and ESP2015-65597-C4-3-R for financial support.